Universal relationship of boson peak with Debye level and Debye-Waller factor in disordered materials

H. P. Zhang,[1] B. B. Fan,[1] J. Q. Wu,[1] W. H. Wang,[2,3] and M. Z. Li[1,*]

[1]*Department of Physics, Beijing Key Laboratory of Opto-Electronic Functional Materials & Micro-Nano Devices, Renmin University of China, Beijing 100872, China*

[2]*Institute of Physics, Chinese Academy of Sciences, Beijing 100190, China*

[3]*Songshan Lake Materials Laboratory, Dongguan, Guangdong 523808, China*

(Received 16 October 2019; revised 29 June 2020; accepted 17 August 2020; published 16 September 2020)

Due to the topological disorder, glass displays an anomalous vibrational density of states beyond the Debye model, i.e., formation of boson peaks, which is fundamental for understanding many glassy physical properties. However, the understanding of the boson peak remains notoriously complex and is a topic of hot debate. Here we report a universal quantitative relation between boson peak intensity and the Debye level of transverse phonons in different glasses, confirming the intrinsic link between boson peaks and transverse phonons. Moreover, an equation is derived for the boson peak intensity and Debye-Waller factor, indicating that boson peaks are fundamentally determined by the Debye-Waller factor. These findings could clarify some controversial issues and reveal a common basis for high-frequency boson peak dynamics ($\sim 10^{12}$ Hz), short-time β processes ($10^3 \sim 10^6$ Hz), and long-time α processes ($10^{-4} \sim 10^3$ Hz) in disordered materials.

DOI: 10.1103/PhysRevMaterials.4.095603

I. INTRODUCTION

In crystalline materials, the normal modes can be quantized as phonons and the vibrational density of states (VDOS) at low frequencies obeys the Debye squared-frequency law, $D(\omega) = A_D\omega^2$, where $D(\omega)$ and A_D are the VDOS and the Debye level, respectively. In disordered materials, however, the scaled VDOS, $D(\omega)/\omega^2$, does not stay constant but goes through a maximum at around a few terahertz. This indicates the existence of an excess VDOS beyond the Debye model, known as the boson peak, which is observed universally in disordered materials [1–7]. The boson peak is believed to be key to a fundamental understanding of the vibrational states of disordered materials. Although much effort has been devoted to it, understanding of the boson peak still remains a serious puzzle in condensed-matter physics and materials science.

The boson peak can be characterized in terms of the boson peak frequency ω_{BP} and the intensity, defined as $I_{BP} = D(\omega_{BP})/\omega_{BP}^2$. Both experiments and numerical simulations find that with an increase in the pressure, the boson peak frequency shifts towards a higher frequency and the peak intensity becomes weaker [8,9]. While some experimental measurements show that boson peak intensity after scaling by the Debye level, that is, I_{BP}/A_D, increases with an increase in pressure [8], several other studies find that I_{BP}/A_D is independent of pressure [2,3,6,9], suggesting that I_{BP} characterizing the excess VDOS could be proportional to A_D characterizing the acoustic phonon modes.

The boson peak intensity in glasses also varies considerably with temperature and processing history, e.g., cooling rate and thermal/mechanical aging/rejuvenation [10,11]. It is found that hyperquenched silicate glass shows a higher I_{BP} with respect to the annealed glass [10]. While the boson peak intensity I_{BP} becomes stronger with increasing temperature in some glasses [11], the boson peak in silica glass exhibits the opposite temperature dependence [12]. Meanwhile, I_{BP} is found to be proportional to A_D in some cases [10,11], whereas the linear relation fails to be observed for I_{BP} and A_D in other cases [12]. Recently it was found in a binary reactive mixture that the scaling between I_{BP} and A_D holds for high-temperature liquids but breaks down for low-temperature glasses [5,13]. On the other hand, it was found that the boson peak intensity increases with a decrease in the fragility of a glass-forming liquid [2]. Recent experimental observations also show that the boson peak intensity in metallic glass decreases in the isothermal aging process at a constant temperature [14]. Thus it is intriguing to explore what underlying physical factors control the boson peak in disordered materials.

Recently, the boson peak in a $Ni_{30}Zr_{70}$ metallic glass was found to be closely related to the time-dependent fluctuations of local environments of atoms [15]. In addition, numerical simulations of a $Cu_{50}Zr_{50}$ metallic glass show that atoms residing in different types of Voronoi polyhedra display different boson peak intensities, and a structural parameter of orientational order for the Voronoi polyhedra was proposed which scales linearly with the boson peak intensity [16]. Thus revealing the underlying physical basis for the structural fluctuation and orientational order of local atomic structures in metallic glasses will be essential for understanding the nature of the boson peak.

In this article we tackled this challenging task by using numerical simulations for various metallic glasses (MGs) and analyzing the experimental data of various types of glasses obtained from literature. Explicit relations are derived for the

*Corresponding author: maozhili@ruc.edu.cn

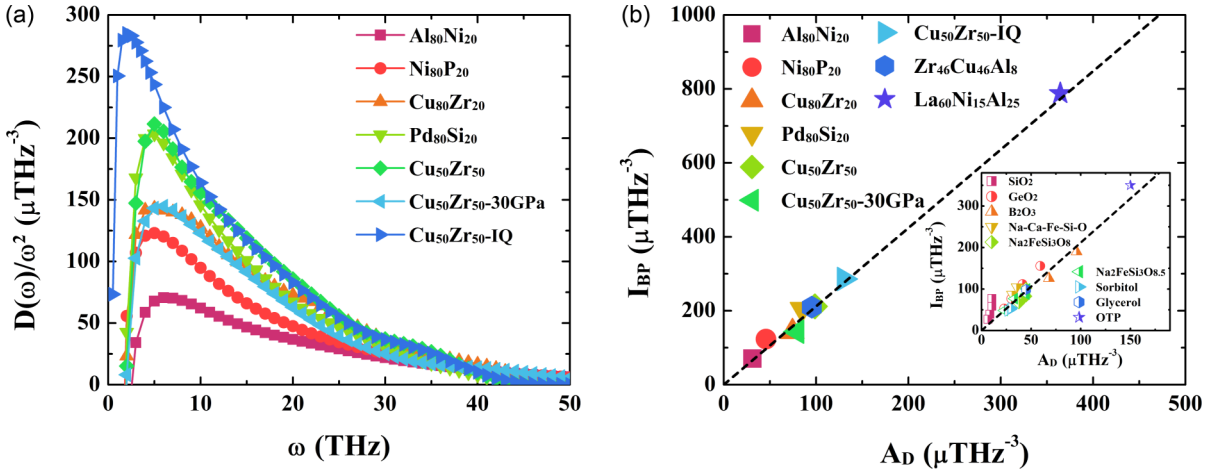

FIG. 1. (a) The reduced VDOS $D(\omega)/\omega^2$ for simulated MG samples at 100 K showing the boson peak. (b) The dependence of the boson peak intensity I_{BP} on the Debye level A_D for simulated MGs (see Supplemental Material [25], Table SI). The dashed line represents the linear fitting of $I_{BP} = C_0 A_D$, where C_0 was fitted about 2.1. The inset in (b) shows the data of $I_{BP} \sim A_D$ obtained from literature for various glasses, including SiO_2 [26,27], GeO_2 [28], B_2O_3 [29], Na-Ca-Fe-Si-O [10], $Na_2FeSi_3O_8$ [9], $Na_2FeSi_3O_{8.5}$ [6], sorbitol [11], glycerol [30], and OTP [31] (see Supplemental Material [25], Table SII). These data satisfy the equation of $I_{BP} = C_0 A_D$ (dashed line). $Cu_{50}Zr_{50}$-IQ in legend denotes the instantaneously quenched $Cu_{50}Zr_{50}$ MG sample (same in other figures).

boson peak intensity and the Debye level of the transverse phonons, the shear modulus, and Debye-Waller factor. These relations are universal for various types of glasses and independent of pressure, processing history, and fragility. These findings explicitly indicate that the boson peak is mostly dominated by the transverse phonons and fundamentally determined by the Debye-Waller factor in disordered materials.

II. MODEL AND METHOD

We performed extensive molecular dynamics (MD) simulations within the LAMMPS [17] software package to prepare and analyze several MGs using the embedded atom method potentials, including $Al_{80}Ni_{20}$, $Ni_{80}P_{20}$, $Cu_{80}Zr_{20}$, $Pd_{80}Si_{20}$, $Cu_{50}Zr_{50}$, $Zr_{46}Cu_{46}Al_8$, and $La_{60}Ni_{15}Al_{25}$ systems [18–23]. In MD simulations, each sample contains 40 000 atoms in a cubic box with periodic boundary conditions applied in three directions. The samples were first equilibrated at 2000 K for 2.0 ns, followed by hyperquenching to 100 K with cooling rate of 1.0×10^{12} K/s, and further relaxed at 100 K for 2.0 ns. The time step was selected as 2.0 fs. The quenching process was performed in an NPT ensemble with zero pressure. To study the effect of pressure and cooling rate on the boson peak, another two $Cu_{50}Zr_{50}$ MG samples were prepared. One was obtained by annealing the hyperquenched $Cu_{50}Zr_{50}$ MG sample for 2.0 ns under a pressure of 30 GPa at 100 K, and the other one was obtained by instantaneously quenching the liquid at 1200 K down to 100 K. Finally, all the samples were relaxed for 10 ps at 100 K under NVT ensemble, and the data were collected for the analysis of structure and dynamics. Here, $D(\omega)$ of the glass is calculated from the Fourier transformation of the velocity autocorrelation function [24,25] (see Supplemental Material [25], Sec. II).

III. RESULTS

Figure 1(a) shows the reduced VDOS of $D(\omega)/\omega^2$ for simulated MGs under various conditions. Boson peak intensities in these samples are significantly different, varying with composition, pressure, and processing history, whereas the boson peak frequencies are very close. In contrast, Fig. 1(b) clearly illustrates that I_{BP} in various MGs under different conditions shows perfect linear dependence on the Debye level A_D (see Supplemental Material [25], Sec. III, for calculation of the Debye level), that is,

$$I_{BP} = C_0 A_D, \tag{1}$$

where $C_0 \approx 2.1$. To check the general validity of this linear relation, we summarized experimental data of I_{BP} and A_D from literature for various glasses, including metal-metalloid glasses, oxide glasses, and molecular glasses [6,9–11,26–31] (see Supplemental Material [25], Table SII). As shown in the inset in Fig. 1(b), the data from literature also satisfy Eq. (1). The relation of $I_{BP} = C_0 A_D$ established over a wide range of values for I_{BP} and A_D is impressive, demonstrating that there exists a universal linear relation between I_{BP} and A_D for almost all glasses. The universal relation suggests that I_{BP}/A_D is independent of composition, pressure, and processing history, as well as the fragility [2]. The boson peak intensity characterizes the excess vibrational modes beyond the Debye model, whereas the Debye level represents the phonon modes within the Debye model. Thus the linear relation of $I_{BP} = C_0 A_D$ clearly shows that the excess modes are intimately connected to the acoustic phonons in disordered materials. We noticed that silica glass exhibits a relatively complex situation. I_{BP} values measured in different experiments are quite different, and a few data deviate from Eq. (1) (see Fig. 1(b) and Supplemental Material [25], Table SII). This could be due to the complex motions of the local tetrahedral units of SiO_4 in silica glass [32]. However, further careful study is necessary for silica glass to check whether this system is special or not. Here, for MGs the boson peak intensity shows perfect linear correlation with the Debye level, suggesting that boson peak modes could be acoustic in disordered materials.

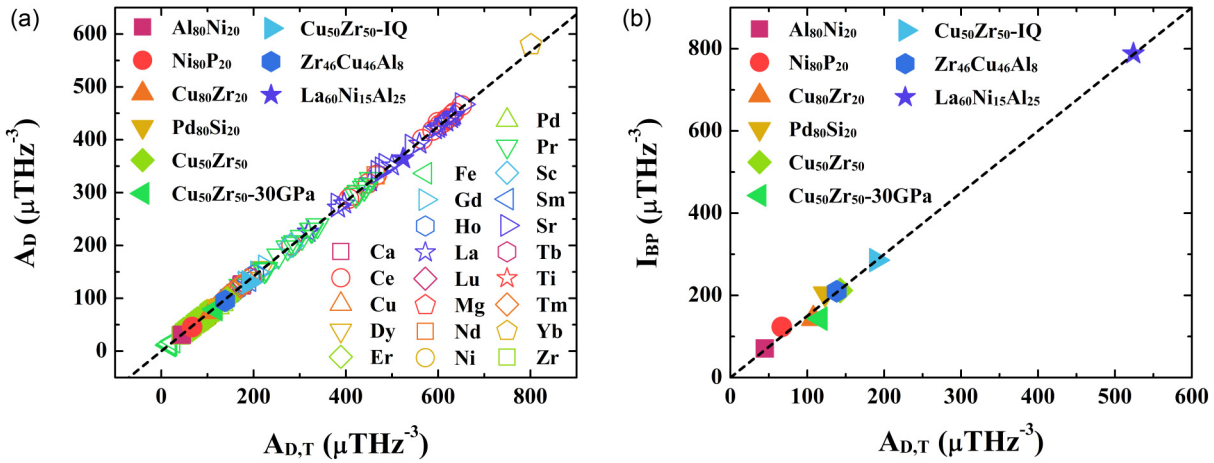

FIG. 2. (a) The Debye level A_D as a function of the transverse Debye level $A_{D,T}$ for ∼200 typical MGs from experimental measurements [34] (open symbols) (see Supplemental Material [25] Table SIII), as well as the simulated MG samples (solid symbols). The dashed line denotes the relation of $A_D \approx 0.7A_{D,T}$ obtained by linear fitting. (b) The dependence of the boson peak intensity I_{BP} on the transverse Debye level $A_{D,T}$ for the simulated MG samples at 100 K. The dashed line represents the derived equation of $I_{BP} = C_1 A_{D,T}$, where $C_1 \approx 1.5$. The simulation data fall exactly on the dashed line.

The acoustic phonon modes consist of two branches of transverse acoustics and one branch of longitudinal acoustics. It is of importance to find out what roles transverse and longitudinal phonons play in the boson peak. Much effort has been devoted to this by clarifying the link between the boson peak frequency and the Ioffe-Regel limit at which the mean free path of the phonons equals their wavelength. While some experimental evidence shows that the boson peak frequency is closely related to the Ioffe-Regel limit of longitudinal phonons for many glasses [33], numerical simulations suggest that the boson peak frequency is equal to the Ioffe-Regel limit for transverse phonons [2]. These contradictory results make the relationship between the boson peak and transverse phonons more elusive. Here this key issue can be clarified by analyzing the relations of the Debye level A_D, the Debye level of the transverse phonons $A_{D,T}$, and longitudinal phonons $A_{D,L}$. According to the longitudinal and transverse sound velocities v_L and v_T measured in experiments for about 200 MGs [34], one can calculate A_D and $A_{D,T}$ (see Supplemental Material [25], Table SIII). Figure 2(a) shows that there exists a perfect linear relation of $A_D \approx 0.7A_{D,T}$. Our simulation data also fall on this linear line. As a result, the relation between I_{BP} and $A_{D,T}$ can be directly derived as

$$I_{BP} = C_1 A_{D,T}, \tag{2}$$

where $C_1 \approx 1.5$. We checked the simulation data of $I_{BP} \sim A_{D,T}$ and found that they follow exactly this linear behavior, as shown in Fig. 2(b). It is known that for MGs, $v_L/v_T \approx 2$ [34] so that $A_{D,T}/A_{D,L} = (v_L/v_T)^3 \approx 8$, indicating that the transverse phonons essentially dominate the Debye level A_D. Thus a quantitative relation is successfully established for the boson peak intensity and transverse phonons which explicitly indicates that the boson peak is mostly dominated by the transverse phonons in disordered materials.

By substituting $A_{D,T} = V_a/2\pi^2 v_T^3$ with $v_T = \sqrt{GV_a/m}$ in Eq. (2), we can also establish an explicit relation for I_{BP} and shear modulus G as

$$I_{BP} = \frac{C_1}{2\pi^2}\left(\frac{m}{GV_a^{1/3}}\right)^{3/2}, \tag{3}$$

where m and V_a are the average atomic mass and atomic volume, respectively. Because shear modulus is a fundamental material property and the key to some fundamental properties in disordered materials [35–37], Eq. (3) establishes explicit relation for the excess vibrational modes and the key mechanical parameters. It is known that shear modulus is sensitive to the pressure and processing history, which has been attributed to visitations of different metabasins in the potential energy landscape (PEL) [38], and the slope of the metabasin in PEL is determined by the shear modulus [39,40]. Therefore Eq. (3) also reveals a simple relation between the boson peak and the properties of PEL. As indicated by Eq. (3), I_{BP} diverges if G goes to zero, which implies that the metabasins become very shallow in PEL. This could correspond to a phase transition from an amorphous elastic phase to a phonon-free one, which has been predicted by recent theories [1].

Based on Eq. (3), we can even link the boson peak intensity to some structural parameters. Recent studies reveal a universal correlation between G and the vibrational Debye-Waller (DW) factor $\langle u^2\rangle$, that is, $G = \frac{C_2 k_B T}{\langle u^2\rangle V_a^{1/3}}$, where k_B is the Boltzmann constant and $C_2 \approx 0.5$ is a universal constant for all glasses [41]. Substituting $G = \frac{C_2 k_B T}{\langle u^2\rangle V_a^{1/3}}$ into Eq. (3), we can obtain

$$I_{BP} = C\left(\frac{m\langle u^2\rangle}{k_B T}\right)^{3/2}, \tag{4}$$

where $C = C_1/2\pi^2 C_2^{3/2} \approx 0.215$ is also a universal constant. Thus Eq. (4) explicitly describes the temperature and DW factor dependence of the boson peak intensity. To check whether the simulated data are consistent with Eq. (4) or not, we calculated $\langle u^2\rangle$ for the simulated MGs (see Supplemental Material [25], Sec. IV). Figure 3 shows that the data of $I_{BP} \sim m\langle u^2\rangle$ exactly follow Eq. (4), once the average atomic

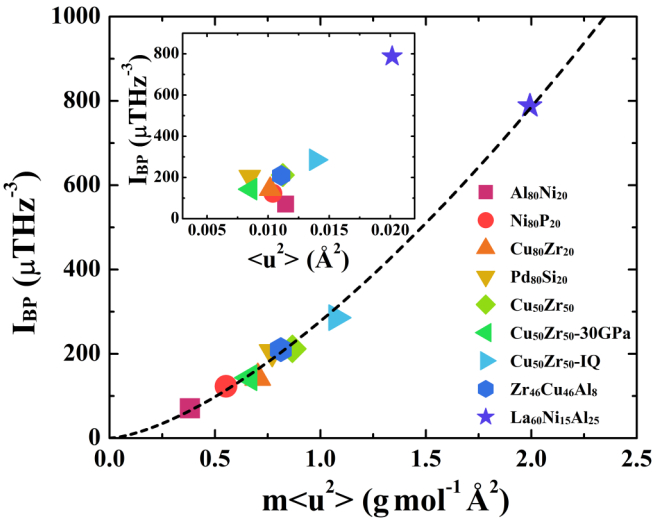

FIG. 3. The boson peak intensity I_{BP} as a function of the mass weighted DW factor $m\langle u^2\rangle$. The dashed line shows Eq. (4): $I_{BP} = C(\frac{m\langle u^2\rangle}{k_BT})^{3/2}$ with $C \approx 0.215$. The inset shows the data of I_{BP} vs $\langle u^2\rangle$, which are scattered.

mass is also considered. The inset in Fig. 3 shows that the data of $I_{BP} \sim \langle u^2\rangle$ are scattered, indicating that the atomic mass has to be considered for different disordered systems. Equation (4) also implies that for a disordered system at temperature T, although the boson peak intensity changes with pressure or processing history, these factors essentially change the DW factor. Thus the DW factor fundamentally determines the boson peak intensity in disordered materials. As to the T-dependent boson peak intensity, because the DW factor also changes with temperature, the ratio of $\langle u^2\rangle/T$ determines the behavior. Thus Eq. (4) quantifies the relative importance of temperature and DW factor for the boson peak intensity in disordered materials.

It is crucial to examine whether Eq. (4) holds for atomic structures in a disordered system, which provides an understanding of the boson peak in atomic scale. So we analyzed the atomic structures of a metallic glass in terms of the Voronoi tessellation method [42–44] and classified them into Voronoi clusters (see Supplemental Material [25], Sec. V). For statistical analysis, Voronoi clusters with fraction more than 1% were selected, and their boson peak intensity I^L_{BP} and local DW factor $\langle u^2\rangle_L$ were calculated. Figure 4(a) shows the dependence of I^L_{BP} on $\langle u^2\rangle_L$ for various atomic clusters in $Cu_{50}Zr_{50}$ and $Al_{80}Ni_{20}$ MGs, respectively. For the same element, the larger the $\langle u^2\rangle_L$ of atomic clusters the higher I^L_{BP} is, consistent with previous simulations [16]. It is also shown that in $Cu_{50}Zr_{50}$ MG, Zr-centered clusters show higher I^L_{BP} than Cu-centered clusters, and in $Al_{80}Ni_{20}$ MG, Ni-centered clusters have higher I^L_{BP} than Al-centered ones. This indicates that elements with larger masses make more contributions to the boson peak intensity. For Cu- and Ni-centered clusters, the data of $I^L_{BP} \sim \langle u^2\rangle_L$ almost collapse together. This is because of very similar atomic masses of Cu and Ni. Thus if the local DW factor is weighted with the element mass $m\langle u^2\rangle_L$, the data of $I^L_{BP} \sim m\langle u^2\rangle_L$ for various atomic clusters collapse on a master curve, exactly following Eq. (4), as shown in Fig. 4(b), indicating that Eq. (4) also holds for local atomic structures in disordered materials. Thus the boson peak intensity is fundamentally determined by the DW factor in both microscopic and macroscopic scale. This finding indicates that all atoms participate in the excess modes associated with the boson peak. The contribution of each atom to the boson peak intensity is mainly determined by its local DW factor. Recent theoretical studies suggest that the boson-peak-related vibrational anomalies arise naturally from the diffusive phonon damping [7], which is induced by spatial fluctuations of elastic constants from the structural disorder in glasses [45,46]. In fact, the heterogeneous shear elasticity of glasses is found to be closely related to the heterogeneous Debye-Waller factor [41]. Thus the above results are consistent with these theoretical studies.

IV. DISCUSSION

Previous simulations reveal that in supercooled liquids the local DW factor exhibits significant spatial heterogeneities which correspond to the β processes and provide an excellent predictor for the subsequent α processes [47,48]. Our

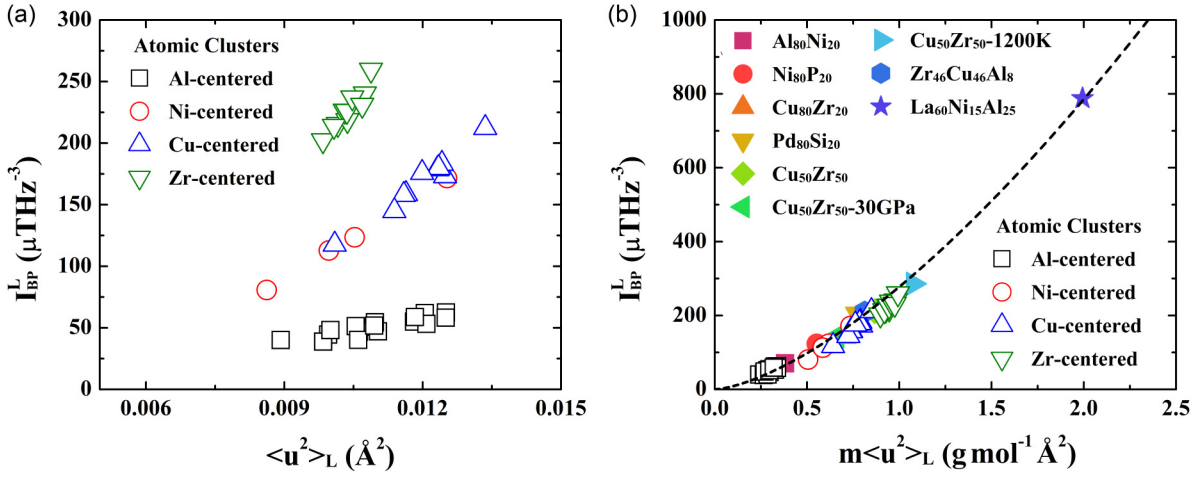

FIG. 4. (a) Local boson peak intensity I^L_{BP} as a function of local DW factor $\langle u^2\rangle_L$. (b) Local boson peak intensity as a function of the mass weighted local DW factor. The dashed line in (b) illustrates the equation of $I^L_{BP} = C(\frac{m\langle u^2\rangle_L}{k_BT})^{3/2}$ with $C \approx 0.215$.

results also show that the DW factor determines the boson peak intensity in disordered materials. Thus the DW factor may be the common basis for glassy dynamics from the high-frequency boson peak, short-time β processes, to long-time α relaxation, indicating that the glassy dynamics in a broad frequency/timescale ($10^{-4} \sim 10^{12}$ Hz) are fundamentally connected. On the other hand, from the PEL perspective, the boson peak, β and α processes are all intimately connected, because α processes correspond to the transitions between metabasins in PEL, and β processes are the elementary hopping between the sub-basins within a metabasin [38–40]. Our results indicate that the boson peak is related to the slope of metabasins in PEL. The above finding reveals the physical origin for the correlation between the boson peak and structural relaxation observed recently in a MG [14]. Our results provide a more general insight into the nature of glass and glass transitions.

As mentioned above, the scaling behavior of the boson peak with the elastic properties remains a topic of hot debate. For example, the scaling between I_{BP} and A_D holds for high-temperature liquids but breaks down for low-temperature glasses in a binary reactive mixture [13]. The universal relation of Eq. (1) suggests that the vibrational dynamics in this binary reactive mixture could be very different from those in metallic glasses and oxide glasses. Moreover, a similar scaling of the boson peak is also observed in a simulated model glass, with different stabilities generated via the swap Monte Carlo method, that is, $I_{BP} \propto A_D$. However, the prefactor is about 3, different from the value of 2.1 [4]. This also suggests that there could exist some other factors that affect the vibrational dynamics in these model glasses with pure repulsive potential and generated via swap Monte Carlo method, which may be fundamentally different from MGs. Thus further studies are highly desirable to elucidate these differences. This may provide new understanding for the underlying mechanism of the vibrational anomaly and the nature of glass. Note that the elastic properties of disordered materials need to be carefully characterized in experiments, since it is found that the anharmonic and relaxational effects may strongly influence the experimentally measured elastic properties, such as sound velocity, which could significantly affect the scaling behavior of the boson peak [49].

It was also found that the scaling between the boson peak and the Debye level is consistent with the Cauchy-like relation [13]. Here we also checked the relation between the scaling and the Cauchy-like relation in MGs. The relation between longitudinal modulus L and shear modulus G of a glass can be generally described as $L = a + bG$, where a and b represent the shift and slope, respectively. The Cauchy-like relation corresponds to the case of $b = 3$. Considering $L = K + 4G/3$, the equation can also be described as $K = a + (b - 4/3)G$, where K is the bulk modulus. Thus the slope b reflects the change of K relative to the change of G, and its value is highly sensitive to the method of sample preparation. That is, cooling rate and pressure could have different effects. For different cooling rates, G in a MG changes a lot but K and the density ρ change little. As a result, b can be less than 2.0 for different cooling rates [41]. On the other hand, upon pressure, K often changes much faster than G so that b can be much larger than 3 [34]. In our work, the change of cooling history for $Cu_{50}Zr_{50}$ corresponds to $b = 1.7$. For $Cu_{50}Zr_{50}$ MG at 30 GPa, b is as large as 27.4, much larger than 3.0. Although the Cauchy-like relation is not obeyed in both cases, the boson peak intensity can be scaled by the Debye level, following Eq. (1). These results imply that the boson peak in MGs is mainly related to G but has little to do with K or a Cauchy-like relation.

It is interesting to investigate the relation between vibrational modes and DW factor to understand how vibrational modes affect the DW factor. In the harmonic approximation, the DW factor can be calculated by integrating the $D(\omega)/\omega^2$ as $\langle u^2 \rangle_{\rm har} = \frac{3k_BT}{m} \int \frac{D(\omega)}{\omega^2} d\omega$. It is found that the value of $\langle u^2 \rangle_{\rm har}$ is very close to the value of $\langle u^2 \rangle$ calculated in MD simulations (see Supplemental Material [25], Sec. IV). Apparently, the integration over the boson peak frequency regime contributes more to the total DW factor. However, one cannot say that the modes in the boson peak regime determine the DW factor. For the local DW factor of atom i, it can be calculated in terms of the eigenvectors of atom i in each mode [50–52]. In previous studies a structural order parameter was constructed from the energy equipartition of all the vibrational modes, $\Psi_i = \sum_\lambda \frac{1}{\omega_\lambda^2} |\mathbf{e}_{\lambda,i}|^2$, where ω_λ and $\mathbf{e}_{\lambda,i}$ are the frequency and eigenvector of atom i participating in mode λ, respectively [50]. It is found that Ψ_i of atom i is essentially equivalent to the local DW factor. It can be seen that all the eigenmodes and eigenvectors of an atom together determine the local DW factor. However, atoms participating in the low-frequency modes with larger eigenvectors might have larger Ψ_i or local DW factors, which correspond to the so-called soft spots identified by analyzing the low-frequency vibrational modes [53]. The soft spots have been found to facilitate the irreversible structural rearrangements, which closely relates to the relaxation dynamics in supercooled liquids and glasses [50,53,54]. However, the low-frequency quasilocalized modes are only part of the local DW factor. That is, the local DW factor of an atom contains more vibrational information, which is consistent with previous studies [50].

V. CONCLUSION

In summary, we reveal the origin of the boson peak in disordered materials by performing MD simulation and analyzing the experimental data from literature. A universal relation between boson peak intensity and transverse Debye level is uncovered that does not depend on thermal history, composition, and pressure, clarifying the relationship between the boson peak and transverse phonons and thereby the relation to mechanical properties such as shear modulus. Finally, the boson peak intensity is found to be fundamentally determined by the DW factor on both atomic and macroscopic scales. Our findings establish a common basis for the fast boson peak dynamics, short-time β processes, and long-time α relaxation processes in disordered materials.

ACKNOWLEDGMENTS

This work was supported by the National Natural Science Foundation of China (Grant No. 51631003) and the MOST 973 Program (Grant No. 2015CB856800).

[1] T. S. Grigera, V. Martín-Mayor, G. Parisi, and P. Verrocchio, Nature (London) **422**, 289 (2003).

[2] H. Shintani and H. Tanaka, Nat. Mater. **7**, 870 (2008).

[3] L. Zhang, J. Zheng, Y. Wang, L. Zhang, Z. Jin, L. Hong, Y. Wang, and J. Zhang, Nat. Commun. **8**, 67 (2017).

[4] L. Wang, A. Ninarello, P. Guan, L. Berthier, G. Szamel, and E. Flenner, Nat. Commun. **10**, 26 (2019).

[5] S. Caponi, S. Corezzi, D. Fioretto, A. Fontana, G. Monaco, and F. Rossi, Phys. Rev. Lett. **102**, 027402 (2009).

[6] A. I. Chumakov, G. Monaco, A. Monaco, W. A. Crichton, A. Bosak, R. Rüffer, A. Meyer, F. Kargl, L. Comez, D. Fioretto, H. Giefers, S. Roitsch, G. Wortmann, M. H. Manghnani, A. Hushur, Q. Williams, J. Balogh, K. Parliński, P. Jochym, and P. Piekarz, Phys. Rev. Lett. **106**, 225501 (2011).

[7] M. Baggioli and A. Zaccone, Phys. Rev. Lett. **122**, 145501 (2019).

[8] K. Niss, B. Begen, B. Frick, J. Ollivier, A. Beraud, A. Sokolov, V. N. Novikov, and C. Alba-Simionesco, Phys. Rev. Lett. **99**, 055502 (2007).

[9] A. Monaco, A. I. Chumakov, G. Monaco, W. A. Crichton, A. Meyer, L. Comez, D. Fioretto, J. Korecki, and R. Rüffer, Phys. Rev. Lett. **97**, 135501 (2006).

[10] A. Monaco, A. I. Chumakov, Y.-Z. Yue, G. Monaco, L. Comez, D. Fioretto, W. A. Crichton, and R. Rüffer, Phys. Rev. Lett. **96**, 205502 (2006).

[11] B. Ruta, G. Baldi, V. M. Giordano, L. Orsingher, S. Rols, F. Scarponi, and G. Monaco, J. Chem. Phys. **133**, 041101 (2010).

[12] B. Rufflé, S. Ayrinhac, E. Courtens, R. Vacher, M. Foret, A. Wischnewski, and U. Buchenau, Phys. Rev. Lett. **104**, 067402 (2010).

[13] S. Corezzi, S. Caponi, F. Rossi, and D. Fioretto, J. Phys. Chem. B **117**, 14477 (2013).

[14] P. Luo, Y. Z. Li, H. Y. Bai, P. Wen, and W. H. Wang, Phys. Rev. Lett. **116**, 175901 (2016).

[15] M. Guerdane and H. Teichler, Phys. Rev. Lett. **101**, 065506 (2008).

[16] J. Yang, Y.-J. Wang, E. Ma, A. Zaccone, L. H. Dai, and M. Q. Jiang, Phys. Rev. Lett. **122**, 015501 (2019).

[17] S. Plimpton, J. Comp. Phys. **117**, 1 (1995).

[18] G. P. Purja Pun and Y. Mishin, Philos. Mag. **89**, 3245 (2009).

[19] H. W. Sheng, E. Ma, and M. J. Kramer, JOM **64**, 856 (2012).

[20] M. I. Mendelev, M. J. Kramer, R. T. Ott, D. J. Sordelet, D. Yagodin, and P. Popel, Philos. Mag. **89**, 967 (2009).

[21] J. Ding, Y.-Q. Cheng, H. Sheng, and E. Ma, Phys. Rev. B **85**, 060201(R) (2012).

[22] Y. Q. Cheng, E. Ma, and H. W. Sheng, Phys. Rev. Lett. **102**, 245501 (2009).

[23] H. W. Sheng, Y. Q. Cheng, P. L. Lee, S. D. Shastri, and E. Ma, Acta Mater. **56**, 6264 (2008).

[24] M. Parrinello and A. Rahman, J. Appl. Phys. **52**, 7182 (1981).

[25] See Supplemental Material at http://link.aps.org/supplemental/10.1103/PhysRevMaterials.4.095603 for details of the calculations, including pair correlation functions, VDOS, Debye level, vibrational DW factor, and local atomic structures.

[26] A. Wischnewski, U. Buchenau, A. J. Dianoux, W. A. Kamitakahara, and J. L. Zarestky, Phys. Rev. B **57**, 2663 (1998).

[27] A. I. Chumakov, G. Monaco, A. Fontana, A. Bosak, R. P. Hermann, D. Bessas, B. Wehinger, W. A. Crichton, M. Krisch, R. Rüffer, G. Baldi, G. Carini Jr., G. Carini, G. D'Angelo, E. Gilioli, G. Tripodo, M. Zanatta, B. Winkler, V. Milman, K. Refson *et al.*, Phys. Rev. Lett. **112**, 025502 (2014).

[28] L. Orsingher, A. Fontana, E. Gilioli, G. Carini, G. Carini, G. Tripodo, T. Unruh, and U. Buchenau, J. Chem. Phys. **132**, 124508 (2010).

[29] D. Engberg, A. Wischnewski, U. Buchenau, L. Börjesson, A. J. Dianoux, A. P. Sokolov, and L. M. Torell, Phys. Rev. B. **59**, 4053 (1999).

[30] J. Wuttke, W. Petry, G. Coddens, and F. Fujara, Phys. Rev. E **52**, 4026 (1995).

[31] A. Tölle, H. Zimmermann, F. Fujara, W. Petry, W. Schmidt, H. Schober, and J. Wuttke, Eur. Phys. J. B **16**, 73 (2000).

[32] U. Buchenau, M. Prager, N. Nücker, A. J. Dianoux, N. Ahmad, and W. A. Phillips, Phys. Rev. B **345**665 (1986).

[33] B. Rufflé, G. Guimbretière, E. Courtens, R. Vacher, and G. Monaco, Phys. Rev. Lett. **96**, 045502 (2006).

[34] W. H. Wang, Prog. Mater. Sci. **57**, 487 (2012).

[35] W. L. Johnson, M. D. Demetriou, J. S. Harmon, M. L. Lind, and K. Samwer, MRS Bull. **32**, 644 (2007).

[36] M. D. Demetriou, M. E. Launey, G. Garrett, J. P. Schramm, D. C. Hofmann, W. L. Johnson, and R. O. Ritchie, Nat. Mater. **10**, 123 (2011).

[37] H. B. Yu, W. H. Wang, and K. Samwer, Mater. Today **16**, 183 (2013).

[38] F. H. Stillinger, Science **267**, 1935 (1995).

[39] Y. Fan, T. Iwashita, and T. Egami, Nat. Commun. **5**, 5083 (2014).

[40] H. Y. Xu, H. W. Sheng, and M. Z. Li, J. Appl. Phys. **123**, 125108 (2018).

[41] J. Ding, Y.-Q. Cheng, H. Sheng, M. Asta, R. O. Ritchie, and E. Ma, Nat. Commun. **7**, 13733 (2016).

[42] V. A. Borodin, Philos. Mag. A **79**, 1887 (1999).

[43] H. W. Sheng, W. K. Luo, F. M. Alamgir, J. M. Bai, and E. Ma, Nature (London) **439**, 419 (2006).

[44] F. X. Li and M. Z. Li, J. Appl. Phys. **122**, 225103 (2017).

[45] A. Marruzzo, W. Schirmacher, A. Fratalocchi, and G. Ruocco, Sci. Rep. **3**, 1407 (2013).

[46] H. Mizuno and A. Ikeda, Phys. Rev. E **98**, 062612 (2018).

[47] A. Widmer-Cooper and P. Harrowell, Phys. Rev. Lett. **96**, 185701 (2006).

[48] L. Larini, A. Ottochian, C. De Michele, and D. Leporini, Nat. Phys. **4**, 42 (2008).

[49] G. Baldi, A. Fontana, G. Monaco, L. Orsingher, S. Rols, F. Rossi, and B. Ruta, Phys. Rev. Lett. **102**, 195502 (2009).

[50] H. Tong and N. Xu, Phys. Rev. E **90**, 010401(R) (2014).

[51] E. Lerner, G. Düring, and E. Bouchbinder, Phys. Rev. Lett. **117**, 035501 (2016).

[52] H. Mizuno, H. Shiba, and A. Ikeda, Proc. Nat. Aca. Sci. USA **114**, 9767 (2017).

[53] M. L. Manning and A. J. Liu, Phys. Rev. Lett. **107**, 108302 (2011).

[54] A. Widmer-Cooper, H. Perry, P. Harrowell, and D. R. Reichman, Nat. Phys. **4**, 711 (2008).